Received: 15 September 2022 | Revised: 11 November 2022 | Accepted: 14 November 2022

DOI: 10.1111/pim.12957

ORIGINAL ARTICLE

Parasite Immunology WILEY

Th2 and metabolic responses to nematodes are independent of prolonged host microbiota abrogation

Luis E. Elizalde-Velázquez[1] | Ivet A. Yordanova[1] | Wjatscheslaw Liublin[2] | Joshua Adjah[1] | Ruth Leben[1,2] | Sebastian Rausch[1] | Raluca Niesner[2] | Susanne Hartmann[1]

[1]Institute of Immunology, Center for Infection Medicine, Freie Universität Berlin, Berlin, Germany

[2]Biophysical Analytics, German Rheumatism Research Center, Leibniz Institute and Dynamic and Functional in vivo Imaging, Veterinary Medicine, Freie Universität Berlin, Berlin, Germany

Correspondence
Susanne Hartmann, Institute of Immunology, Center for Infection Medicine, Freie Universität Berlin, Berlin, Germany.
Email: susanne.hartmann@fu-berlin.de

Present address
Ivet A. Yordanova, Centre for Biological Threats and Special Pathogens, Robert Koch Institute, Berlin, Germany.

Funding information
Deutsche Forschungsgemeinschaft, Grant/Award Numbers: HA 2542/8-1, HA 2542/12-1

Abstract

Antibiotic treatment can lead to elimination of both pathogenic bacteria and beneficial commensals, as well as to altered host immune responses. Here, we investigated the influence of prolonged antibiotic treatment (Abx) on effector, memory and recall Th2 immune responses during the primary infection, memory phase and secondary infection with the small intestinal nematode *Heligmosomoides polygyrus*. Abx treatment significantly reduced gut bacterial loads, but neither worm burdens, nor worm fecundity in primary infection were affected, only worm burdens in secondary infection were elevated in Abx treated mice. Abx mice displayed trends for elevated effector and memory Th2 responses during primary infection, but overall frequencies of Th2 cells in the siLP, PEC, mLN and in the spleen were similar between Abx treated and untreated groups. Gata3^{+} effector and memory Th2 cytokine responses also remained unimpaired by prolonged Abx treatment. Similarly, the energy production and defence mechanisms of the host tissue and the parasite depicted by NAD(P)H fluorescence lifetime imaging (FLIM) did not change by the prolonged use of antibiotics. We show evidence that the host Th2 response to intestinal nematodes, as well as host and parasite metabolic pathways are robust and remain unimpaired by host microbiota abrogation.

KEYWORDS
antibiotic, FLIM, *H. polygyrus*, metabolism, microbiota, NAD(P)H, Th2 response

1 | INTRODUCTION

Antibiotics are a common treatment strategy against bacterial infections worldwide. Nevertheless, antibiotic treatment can exert a negative influence on both pathogenic bacteria and on host intestinal commensals. An intact host microbiome and microbiota sensing are important for functional immune responses against non-microbial targets, shown for example for vaccinations against influenza.[1] In this sense, we therefore consider it important to assess whether control of a helminth infection could also be affected by a prolonged antibiotic treatment, as no information besides effects of short antibiotic treatment or usage of germ-free mice have been reported in the context of an acute helminth infection.[2–4]

Previous studies have shown that commensal bacterial communities are implicated in regulating host Th2 immunity.[5,6] Indeed, RORγt-expressing regulatory T cells (Treg) driven by microbiota signalling restrict Th2 responses to the murine gut nematode *Heligmosomoides polygyrus* (*H. polygyrus*).[7] Moreover, in line with these findings, we have previously shown that *H. polygyrus*-infected germ-free mice harbour significantly fewer intestinal RORγt$^+$ Treg cells and display overall poor IL-10 production. On the other hand, the absence of microbes in germ-free mice was contrasted by a normal expansion of effector Th2 cells during acute nematode infection.[2] However, whether the host microbiota influences the formation and maintenance of memory Th2 cell responses and how perturbations in host intestinal commensals following prolonged antibiotic treatment potentially affect Th2 responses to a challenge infection remain unaddressed.

In specific pathogen-free (SPF) mice, in the context of immunological memory, we have previously demonstrated that 8 weeks following cure of a primary *H. polygyrus* infection, mice harbour highly functional tissue-resident memory Th2 cells in the small intestinal lamina propria (siLP) and the peritoneal cavity.[8] Moreover, the host peritoneal cavity also appears to function as a prominent site for the initial expansion and parasite-specific reactivation of peritoneal-resident memory Th2 cells early on following a *H. polygyrus* challenge infection.[9] Beyond the gut environment, functional and protective memory Th2 cells have also been found to accumulate in the lungs of mice infected with the tissue-migratory nematode *Nippostrongylus brasiliensis*.[10,11] Thus, Th2 cell-driven immune responses dominate the primary, memory and recall responses to parasitic nematodes. Yet, how the metabolism of the host immune system changes during infection with *H. polygyrus* and upon prolonged interference with the host microbiota, remains poorly studied. By using fluorescence lifetime imaging (FLIM) of the co-enzymes NADH and NADPH—conserved across species—in live infected duodenal tissue,[12] we are able to explore the activity of specific metabolic pathways related to energy production and to defence using NADPH oxidases activation, both in host and in parasite, as an additional parameter to the characterization of immune responses.

Here, we therefore investigated how antibiotics potentially affect the formation, maintenance and recall responses of host memory Th2 cells. In parallel, we evaluated possible changes in the activity of different metabolic pathways in the parasite and host gut tissue via FLIM of the co-enzymes NADH and NADPH, present in all cells and involved in key metabolic processes.[12]

2 | MATERIALS AND METHODS

2.1 | Animal handling, nematode infection and antibiotic treatment

Wild-type female C57BL/6 mice aged 8–10 weeks were purchased from Janvier Labs (Saint-Berthevin, France). All animals were maintained under SPF conditions and were fed standard chow *ad libidum*. For antibiotic treatment, ampicillin (0.5 mg/ml), gentamycin (0.5 mg/ml), neomycin (0.5 mg/ml) and vancomycin (0.25 mg/ml) were added to the drinking water of the designated cages of mice for the entire duration of the experiment, starting 14 days before primary nematode infection (**Abx** groups). The remaining mice were given normal drinking water (**SPF** groups). *H. polygyrus* was maintained by serial passage in C57BL/6 mice (H0099/13). Both SPF and Abx mice assigned to primary or secondary infection were infected with 225 third-stage infective (L3) *H. polygyrus* larvae via oral gavage in 200 µl drinking water. For curative treatment of primary infection, mice were treated as previously described.[8,9] On indicated dissection days, the mice were sedated via isofluorane inhalation, followed by cervical dislocation. For the evaluation of female worm fecundity, individual female *H. polygyrus* worms were isolated from the small intestines of infected mice and were plated out in a 96-well plate containing 150 µL/well of cRPMI medium. The worms were incubated at 37°C for 24 h, after which the numbers of eggs excreted by single worms were counted using a Neubauer chamber under a light microscope. All animal experiments were performed in accordance with the National Animal Protection Guidelines and approved by the German Animal Ethics Committee for the Protection of Animals (LAGeSO, G0176/20).

2.2 | Preparation of single cell suspensions and in vitro stimulation

The isolation of spleen, peritoneal exudate cells (PEC), siLP and mesenteric lymph nodes (mLN) cells was performed as previously described.[8,9] All cell suspensions were counted using a CASY automated cell counter (Roche-Innovatis, Reutlingen, Germany). For in vitro stimulation, 2×10^6 of spleen, PEC, siLP or mLN cells were plated out in 200 µl of RPMI medium containing 10% FCS, 100 U/ml penicillin and 100 µg/ml streptomycin. Phorbol-12-myristate-13-acetate (PMA) and Ionomycin were then added at a concentration of 1 µg/ml for 0.5 h. Finally, brefeldin A was supplemented in a 1000-fold dilution and cells were kept under stimulating conditions at 37°C for 3.5 h.

2.3 | Flow cytometry

The antibodies used for the staining and detection of cell surface and intracellular markers are described in Table S1. Dead cells were stained and excluded using an eF506 fixable viability dye (ThermoFischer, Waltham, USA). For intracellular staining of cytokines and transcription factors, cells were fixed and permeabilized using the eBioscience Foxp3/Transcription Factor Fixation/Permeabilization Kit. Samples were acquired on an Aria cell sorter using identical instrument settings among the different experiments (BD Biosciences, Heidelberg, Germany). The results were analysed using the FlowJo software Version 10 (Tree star Inc., Ashland, OR, USA).

2.4 | Bacterial DNA isolation from faeces

For bacterial DNA isolation and quantification of total intestinal bacterial loads, fresh faecal pellets were collected from individual cured and challenged mice and were flash frozen in liquid nitrogen for later processing. Frozen faecal pellets were later thawed and weighed at room temperature, and faecal DNA was isolated using the innuPREP Stool DNA Kit protocol, according to the manufacturer's instructions (Analytik Jena, Berlin, Germany). DNA concentrations and purity were assessed on a Nanodrop (ThermoFischer Scientific, MA, USA).

2.5 | Real-time PCR (RT-PCR)

Absolute quantification of bacterial DNA was determined via RT-PCR using 10 ng of bacterial DNA and FastStart Universal SYBR Green Master Mix (Roche). The primer sequences used for bacterial DNA amplification were UniF334 (5′-ACTCCTACGGGAGGCAGCAGT-3′) and UniR514 (5′-ATTACCGCGGCTGCTGGC-3′).[13] Absolute quantification/fit point analysis was performed by the Roche Light Cycler 480 software.

2.6 | Detection of antigen-specific antibodies in serum

H. polygyrus excretory-secretory molecule (HES)-specific IgG1 and IgE antibodies were measured via ELISA in mice serum. Briefly, 96-well plates were coated with 10 μg/ml of HES and were incubated with serial dilutions of serum samples. Bound antibody isotypes were detected using HRP-conjugated anti-mouse IgG1 and IgE antibodies from Mouse Uncoated ELISA Kits (ThermoFischer Scientific, Vienna, Austria). All samples were run in duplicates and presented as ODs. Absorbance was measured on a Biotek Synergy H1 Hybrid Reader at a 450 nm wavelength.

2.7 | Two-photon fluorescence lifetime imaging (FLIM)

The two-photon fluorescence lifetime imaging experiments were carried on a specialized commercial laser scanning microscope (TriMScope II, LaVision Biotec, Miltenyi, Bielefeld, Germany), as previously described,[14] with a Ti:Sa laser (80 MHz, 140 fs pulses, Chameleon Ultra II, Coherent, Duisburg, Germany) tuned at 760 nm for NAD(P)H excitation. The beam was focused into the sample by a water-immersion objective (20×, NA 1.05, Apochromat, Olympus, Hamburg Germany). NAD(P)H fluorescence was collected in the range 466 ± 30 nm by the detector (TCSPC, LaVision Biotec) with 55-time bin, over at least 9 ns. The acquired images were typically 500 × 500 μm^2 (505 × 505 pixels). Freshly excised murine duodenum samples were cut open, glued on a Petri dish containing PBS medium with 10% FCS, with the luminal part facing the objective lens. We imbedded the samples in low-melting agarose (0.7%–1%) to preserve villi orientation. The Petri dish was kept at 37°C using a heating plate, to ensure in vivo-like NAD(P)H-dependent metabolic activity both in host tissue and in nematodes.[12] Keeping the Petri dish on ice, at 4°C, resulted in lack of fluorescence signal upon excitation at 760 nm, detected at 466 ± 30 nm, in both intestinal tissue of the host and in nematode tissue, confirming the NAD(P)H specificity of the fluorescence used for FLIM evaluation.

TABLE 1 Most abundant NAD(P)H-dependent enzymes in murine cells and *Heligmosomoides polygyrus*[12,16]

Abbreviation	Full name
NAN	Pixel could not be allocated
FREE NAD(P)H	Unbound
MDH	Malate dehydrogenase
HADH	Hydroxyacyl-coenzyme-A dehydrogenase
LDH	Lactate dehydrogenase
G6PDH	Glucose-6-phosphate dehydrogenase
SDH (NADH)	Sorbitol dehydrogenase
GAPDH	Glyceraldehyde-3-phosphate dehydrogenase
IDH	Isocitrate dehydrogenase
SDH (NADPH)	Sorbitol dehydrogenase
PDH/CTBP1	Pyruvate dehydrogenase/C-terminal binding protein 1 (nuclear)
iNOS	Inducible nitric oxide synthase
ADH	Alcohol dehydrogenase
NOX	Activated NADPH oxidation

2.8 | Phasor-analysis of time-domain FLIM-data and enzyme allocation

The time-domain fluorescence lifetime data were analysed as previously described.[14] In brief, the photon arrival histogram was transformed into the normalized phase domain by computing the discrete Fourier transform, resulting in a phasor plot. Each pixel in the phasor plot was assigned to one of the thirteen most abundant NAD(P)H-dependent enzymes (from RNASeq data of both mammal cells[14,15] (Table 1)) or unbound NAD(P)H and transferred back to space domain to create an enzyme map. Similar binding sites of NAD(P)H were grouped to estimate preference for the following metabolic pathways: anaerobic glycolysis/β-oxidation of fatty acids, aerobic glycolysis/OxPhos and oxidative burst (NADPH oxidases (NOX/DUOX) activation). The length of the vector pointing from free/unbound NAD(P)H towards the position of the lifetime of the assigned enzyme gave the general metabolic activity (activity map): 0% (metabolic inactivity, only free NAD(P)H) to 100% (highly active, complete binding to the enzymes).

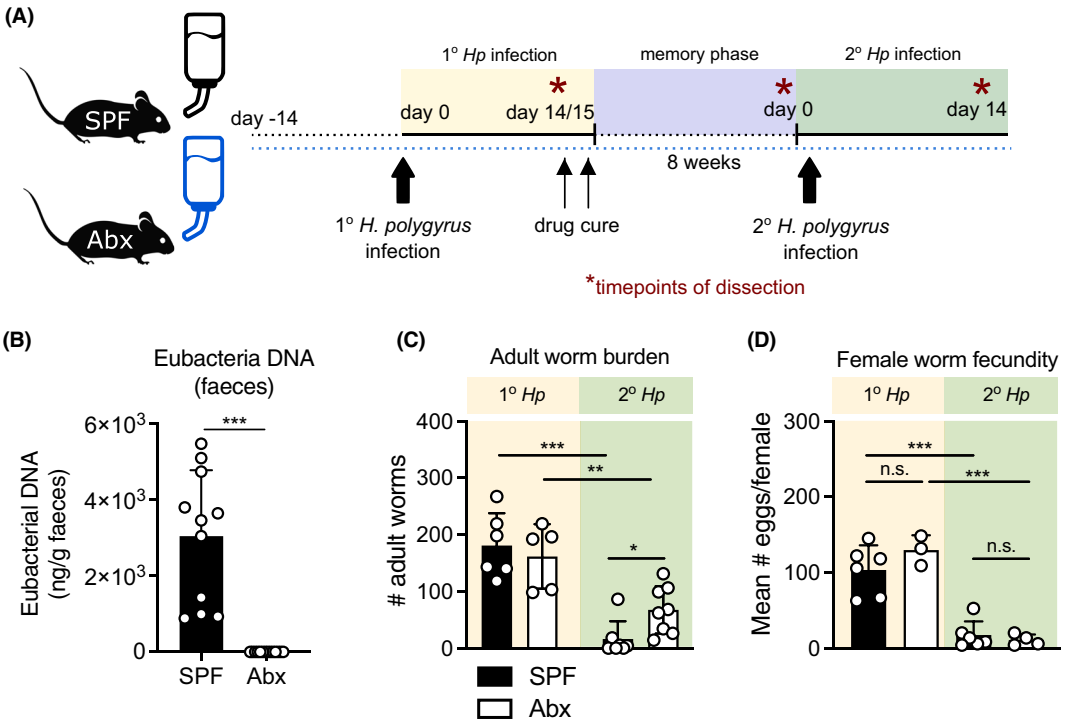

FIGURE 1 Host control of primary and challenge nematode infections remains unimpaired by prolonged antibiotic treatment. (A) Experimental set-up. Briefly, mice were allocated to receive either normal drinking water (SPF) or antibiotic-treated water (Abx) starting 14 days before primary *Heligmosomoides polygyrus* infection. On day 0, both SPF and Abx mice were orally inoculated with 225 L3 infective stage *H. polygyrus* larvae. On day 14, allocated groups of mice were sacrificed (1° Hp groups). On days 14 and 15 of primary infections, the remaining SPF and Abx mice were then given 2 mg per mouse of pyrantel pamoate in drinking water to clear the infection. Drug-cured mice were then allowed to rest for 8 weeks to enter the memory phase. At 8 weeks post-cure, allocated groups of mice were dissected (memory groups) and the remaining groups were given a challenge *H. polygyrus* infection and were sacrificed 14 days post-challenge (2° Hp groups). (B) Amounts of total Eubacteria DNA in faecal samples from drug-cured and challenged SPF and Abx mice, measured via RT-PCR. (C) Adult worm burdens and (D) female worm fecundity in 1° Hp and 2° Hp SPF and Abx mice. The data were pooled from two independent experiments with $n = 2–4$ per group. Statistical analysis was done using one-way ANOVA combined with Tukey's multiple comparison test. *$p < .05$; **$p < .01$; ***$p < .001$; n.s., not significant

2.9 | Segmentation of the NAD(P)H-FLIM maps

In order to distinguish between host and parasite tissues, we performed image segmentation of the NAD(P)H-fluorescence intensity images using a UNet-based algorithm (Python 3.1), as previously described.[12] The algorithm was trained to identify image areas with high fluorescence signal resembling the structure of villi, classified as host tissue, regions belonging the nematodes, identified based on their coiled structure, and in these areas, regions with high fluorescence signal, classified as nematode tissue with high enzymatic activity.

2.10 | Statistical analysis

Statistical analysis of the parasitological, flow cytometry, RT-PCR and ELISA data was performed using GraphPad Prism software version 9.0.1 (La Jolla, CA, USA). Results are displayed as mean ± SD and significance is displayed as *$p < .05$, **$p < .01$, ***$p < .001$. Results were tested for normal distribution using the Shapiro–Wilk normality tests, followed by ANOVA, Kruskal–Wallis combined with Tukey's or Dunn's multiple comparison testing, or a Mann–Whitney *U* test.

3 | RESULTS

3.1 | Reduced bacterial loads but no effect on worm burden and fecundity following Abx treatment

To assess the importance of host gut microbes for the formation, maintenance and functionality of effector and memory Th2 responses and control of *H. polygyrus* infection, groups of mice were given either normal drinking water (SPF) or drinking water with an antibiotic cocktail (Abx) starting 14 days prior to *H. polygyrus* infection. Abx mice were kept under Abx treatment throughout the entire duration of the experiment (Figure 1A). To confirm the temporary abrogation of host microbiota, we firstly quantified total Eubacteria DNA levels in faecal samples of individual SPF and Abx mice, demonstrating a significant reduction of bacterial DNA in mice given an Abx regimen and thus confirming the efficient removal of host commensals (Figure 1B).

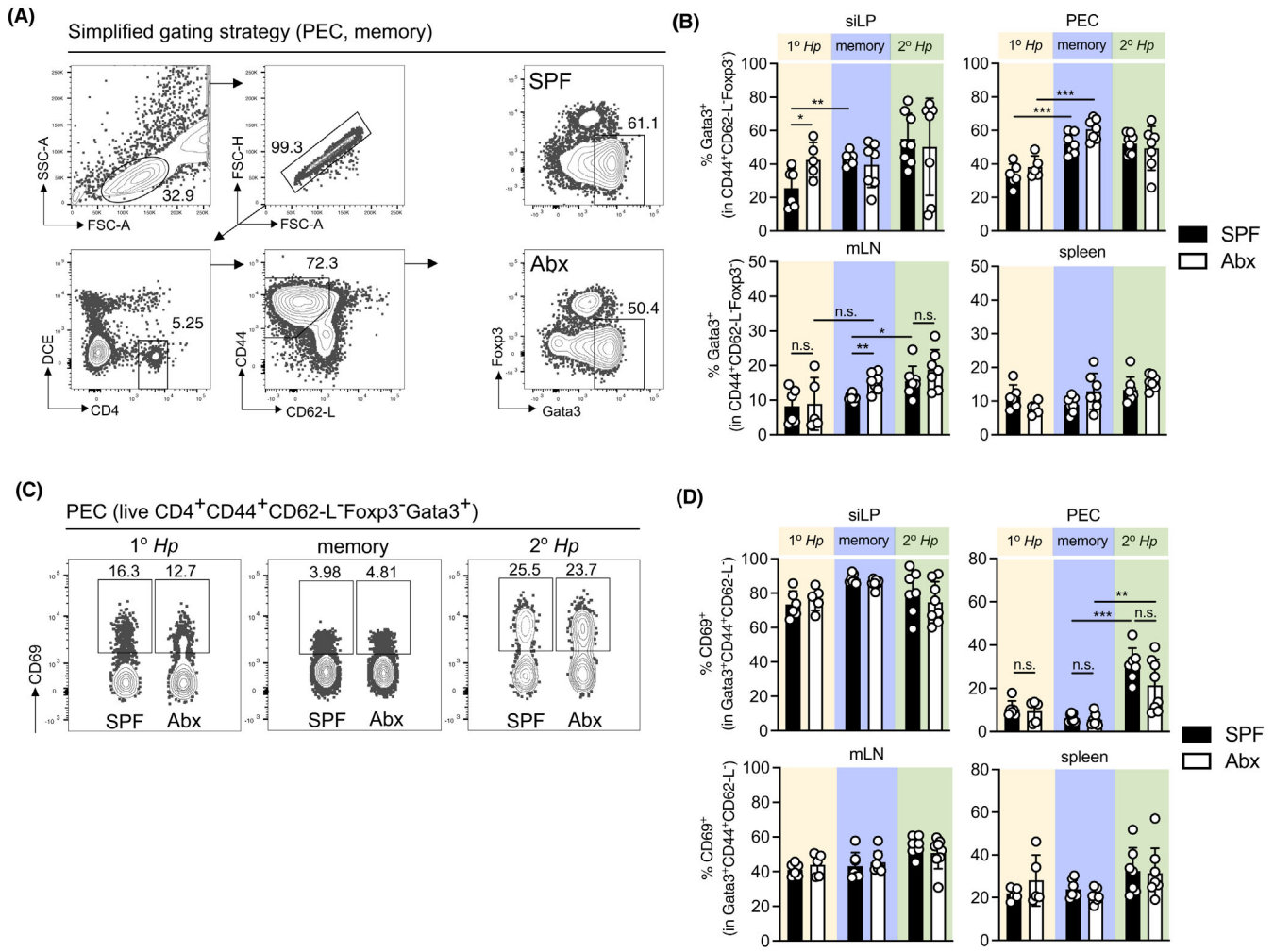

FIGURE 2 Prolonged antibiotic treatment exerts a minor effect on effector and memory Th2 responses in mice following primary and challenge *Heligmosomoides polygyrus* infection. (A) Simplified gating strategy used for the detection of $Gata3^{+}CD44^{+}CD62\text{-}L^{-}Foxp3^{-}$ Th2 cells. (B) Frequencies of Th2 cells in the small intestinal lamina propria (siLP), peritoneal exudate cells (PEC), mesenteric lymph nodes (mLN) and spleen. (C) Representative concatenated plots of CD69 expression in Th2 cells of SPF and Abx mice. (D) Frequencies of $CD69^{+}$ Th2 cells in siLP, PEC, mLN and spleen. The data were pooled from two independent experiments with $n = 2$–4 per group. Statistical analysis was done using one-way ANOVA combined with Tukey's multiple comparison test. $^{*}p < .05$; $^{**}p < .01$; $^{***}p < .001$; n.s., not significant

Comparing primary (1° Hp) to secondary (2° Hp) infections in SPF and Abx mice, next we could show that while adult worm burdens were comparable between the two 1° Hp groups, 2° Hp Abx mice harboured higher numbers of adult worms per small intestine compared with SPF mice (Figure 1C). Nevertheless, significant reductions in adult worm burdens were evident in both SPF and Abx groups, indicative of strong control of challenge *H. polygyrus* infection, regardless of antibiotic treatment. Similarly, female worm fecundity indicated that while antibiotic treatment exerts no significant effect on the numbers of eggs excreted per female worm, SPF and Abx mice display comparable strong reduction in fecundity following secondary *H. polygyrus* infection, compared with primary-infected mice (Figure 1D). In conclusion, prolonged antibiotic treatment of mice did lead to significantly reduced bacterial loads, but only adult worm burden during secondary infection was significantly increased in Abx mice compared to SPF mice.

3.2 | SPF and Abx mice display comparable effector and memory Th2 responses following primary and secondary *H. polygyrus* infection

Next, we asked whether prolonged antibiotic treatment exerts negative effects on the formation, maintenance and recall responses of memory Th2 cells after drug cure of primary nematode infection and following a challenge infection 8 weeks post-cure. Here, while Abx mice displayed elevated effector and memory $Gata3^{+}$ Th2 cell frequencies during primary *H. polygyrus* infection at day 14 post-infection in the small intestinal lamina propria (siLP) and during the memory phase in the mesenteric lymph nodes (mLN), overall frequencies of Th2 populations were comparable between SPF and Abx mice following primary infection, during the memory phase and following secondary nematode infection in the siLP, peritoneal exudate cells (PEC), mLN and in the spleen (Figure 2A,B).

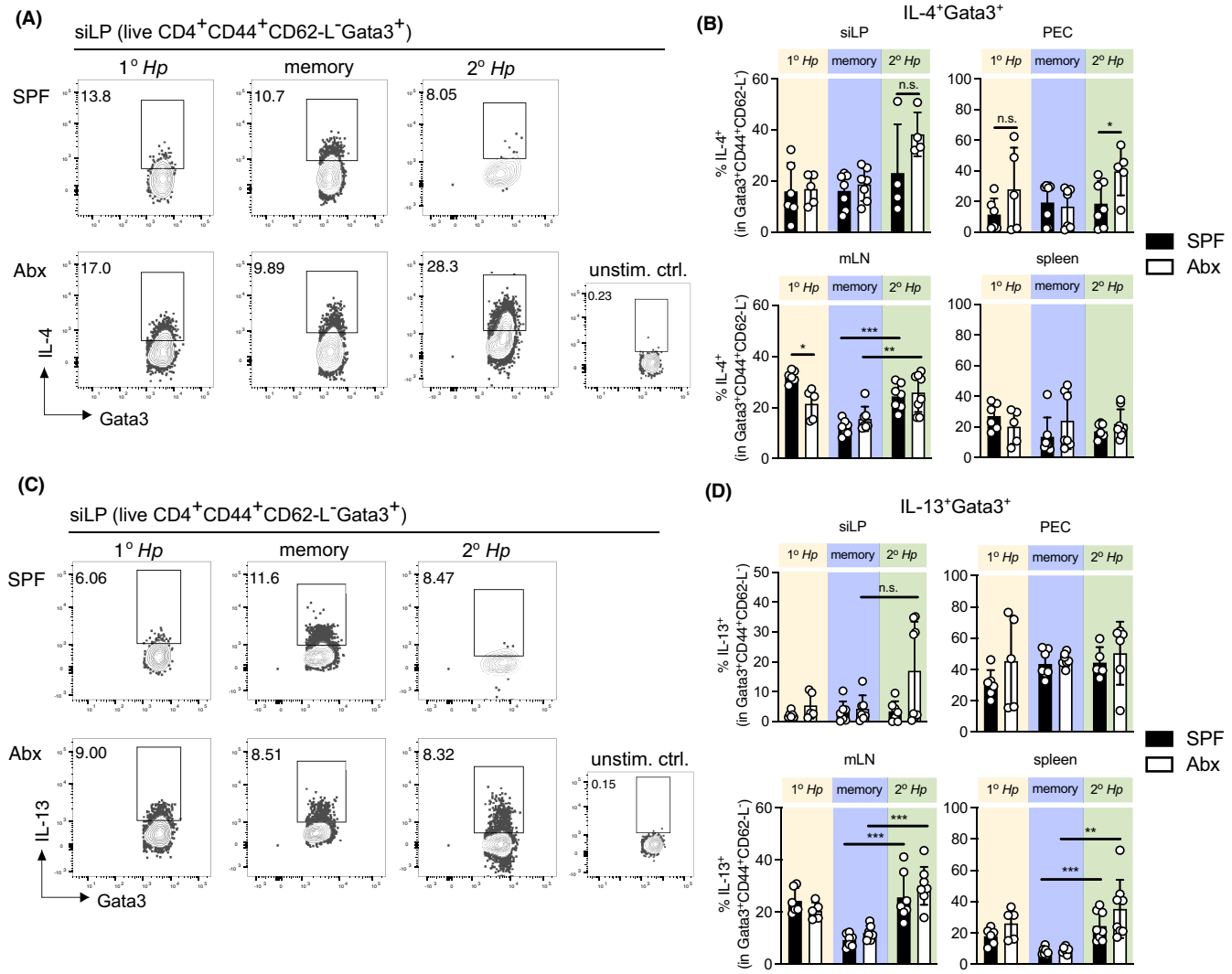

FIGURE 3 SPF and Abx mice show comparable memory Th2 cell formation and Th2 recall responses to a secondary nematode infection. (A) Representative FACS plots showing IL-4$^+$ Th2 cells following in vitro PMA/Ionomycin stimulation and (B) frequencies of IL-4$^+$ Th2 cells in siLP, PEC, mLN and siLP. (C) Representative FACS plots of IL-13$^+$ Th2 cells following in vitro PMA/Ionomycin stimulation and (D) frequencies of IL-13$^+$ Th2 cells siLP, PEC, mLN and siLP of SPF and Abx mice following primary nematode infection, during the memory phase and following secondary *H. polygyrus* infection. The data were pooled from two independent experiments with $n = 2–4$ per group. Statistical analysis was done using one-way ANOVA combined with Tukey's multiple comparison test. *$p < .05$; **$p < .01$; ***$p < .001$; n.s., not significant

We also assessed the surface expression of the T cell tissue retention and activation marker CD69 on effector and memory Th2 cells in SPF and Abx mice at each timepoint (Figure 2C). In agreement with the comparable Th2 cell frequencies, CD69 expression on Th2 cell populations remained comparable between SPF and Abx mice at each timepoint, despite prolonged antibiotic treatment (Figure 2D). Nevertheless, both SPF and Abx mice displayed significantly elevated peritoneal CD69$^+$Gata3$^+$ Th2 cell frequencies following challenge infection, compared with the memory phase—a response not evident in the other tissue sites and in line with our previous findings on the importance of the host peritoneal compartment for memory Th2 cell reactivation.[9] In summary, prolonged antibiotic treatment has only a minor influence on the formation and activation of effector Th2 cells during primary nematode infection, as well as on the maintenance of memory Th2 cells in drug-cured mice. Thus, this study shows for the first time that the formation, activation and maintenance of host Th2 responses to intestinal parasitic nematodes are robust and remain unimpaired by experimental host microbiota abrogation.

3.3 | Prolonged antibiotic treatment exerts minor effects on effector and memory Th2 cell cytokine competence

Next, we assessed whether IL-4, IL-5 and IL-13 cytokines also remain unimpaired (Figure 3, Figures S1 and S2). Here, we could show that following secondary *H. polygyrus* infection, Abx mice displayed a trend for higher IL-4$^+$Gata3$^+$ Th2 cell frequencies than SPF mice

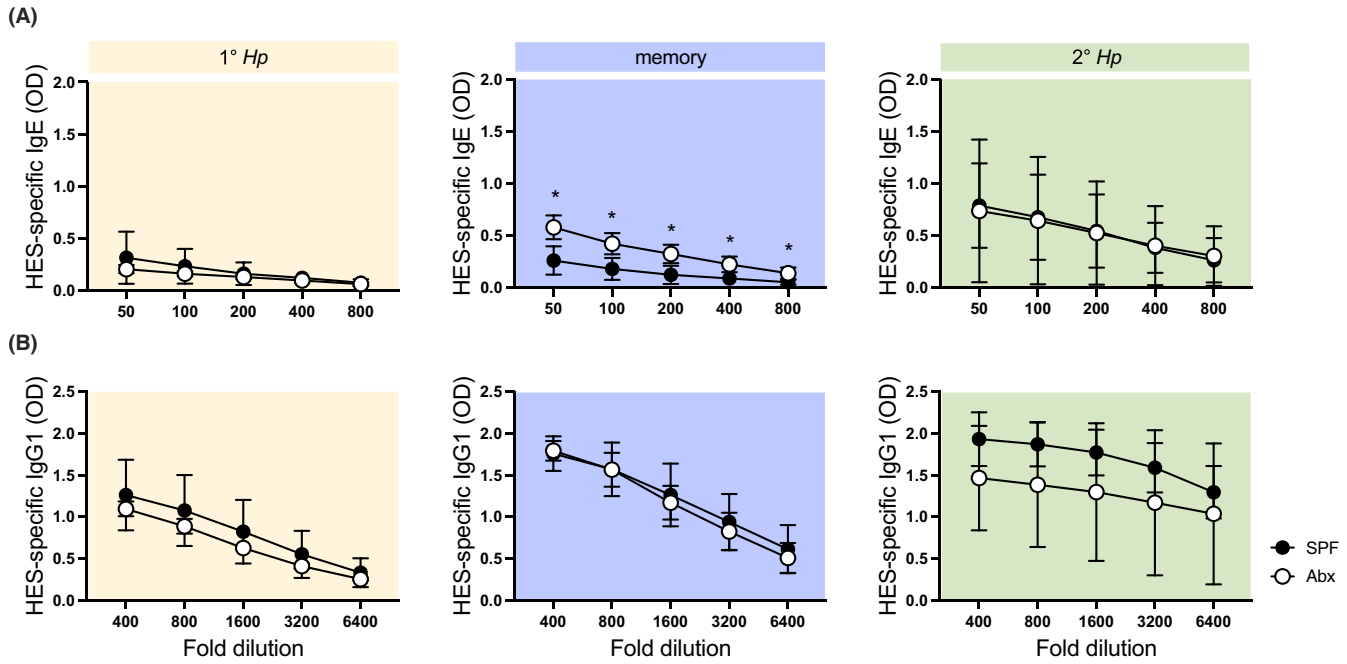

FIGURE 4 IgE and IgG1 antibody responses to *Heligmosomoides polygyrus* excretory-secretory molecules (HES) are not impaired by antibiotic treatment. (A) Plots of serum level of HES-IgE with the serum samples diluted 2-fold from 1:50 to 1:400. (B) Plots of serum levels of HES-IgG1 with serum samples diluted 2-fold from 1:400 to 1:6400. The data were pooled from two independent experiments with $n = 2–4$ per group. Statistical analysis was doing using the Mann–Whitney *U* test. $^{*}p < .05$

(Figure 3A,B). Overall frequencies of IL-4 competent effector and memory Th2 cells, however, were comparable between SPF and Abx mice following primary nematode infection and during the memory phase (Figure 3B). Similarly, IL-13^{+} effector and memory Th2 cells were comparable in SPF and Abx mice at each timepoint of infection (Figure 3C,D). Nevertheless, we observed a clear recall response, where SPF and Abx 2° Hp mice displayed comparable and significant expansion of IL-13^{+} Th2 cells in mLN and spleen, compared with drug-cured mice (Figure 3D). Together, these results therefore confirm that prolonged antibiotic treatment exerts only minor effects on the cytokine competence of both effector and memory Th2 populations in mice infected with a small intestinal parasitic nematode.

3.4 | SPF and Abx mice show similar parasite-specific IgE and IgG1 antibody levels

Changes in gut microbiome caused by antibiotics have been shown to impact antibody responses.[17–20] We therefore additionally checked whether the continuous exposure of mice to antibiotic treatment had any significant impact on antigen-specific IgE and IgG1 levels during the primary, memory, and secondary infection phase in SPF and Abx mice. Overall, we observed that HES-specific IgE and IgG1 levels were similar in both SPF and antibiotic treated mice in primary and secondary infections (Figure 4A,B). Nevertheless, we observe a trend for elevated HES-specific IgE in Abx compared with SPF mice during the memory phase. Overall, these data suggest that despite the lack of a notable impact of prolonged antibiotic treatment had no impact on HES-specific IgG1 formation, it does cause a positive shift in the accumulation of HES-specific IgE in Abx mice following cure of a primary nematode infection.

3.5 | Unchanged metabolic activity in nematodes and host tissue of SPF and Abx mice

While NAD(P)H-dependent metabolism governs energy production and defence mechanisms in host gut and nematodes, the impact of antibiotic treatment on both is still unclear. Using NAD(P)H-FLIM, we were able to assess the general metabolic activity and the specific NAD(P)H-dependent enzymatic activity (Figure 5A, I–III), both in host and nematode tissues. In order to distinguish between host and nematode tissue, with a reliable NAD(P)H signal, that is, signal-to-noise ratio (SNR) > 5 (Figure S3), the fluorescence images were segmented as described in the *Material and Methods* section (Figure 5A, IV). We applied the resulting masks to generate activity and enzyme activity maps for both parasites (Figure 5B, I and IV) and host gut (Figure 5C, I and IV). Based on the enzyme activity maps, we assessed the pixel frequencies of each specific enzyme activity (Figure 5B,C, each II). By clustering the enzymatic activities, we can resolve between no metabolic activity (free NAD(P)H) in blue, anaerobic glycolysis (LDH activity)/β-oxidation of fatty acids (HADH activity) in green, aerobic glycolysis/oxidative phosphorylation—oxPhos (e.g., GAPDH/PDH activity) in yellow, and defence based on oxidative burst (NADPH oxidases activity) in red (Figure 5B,C, each III).

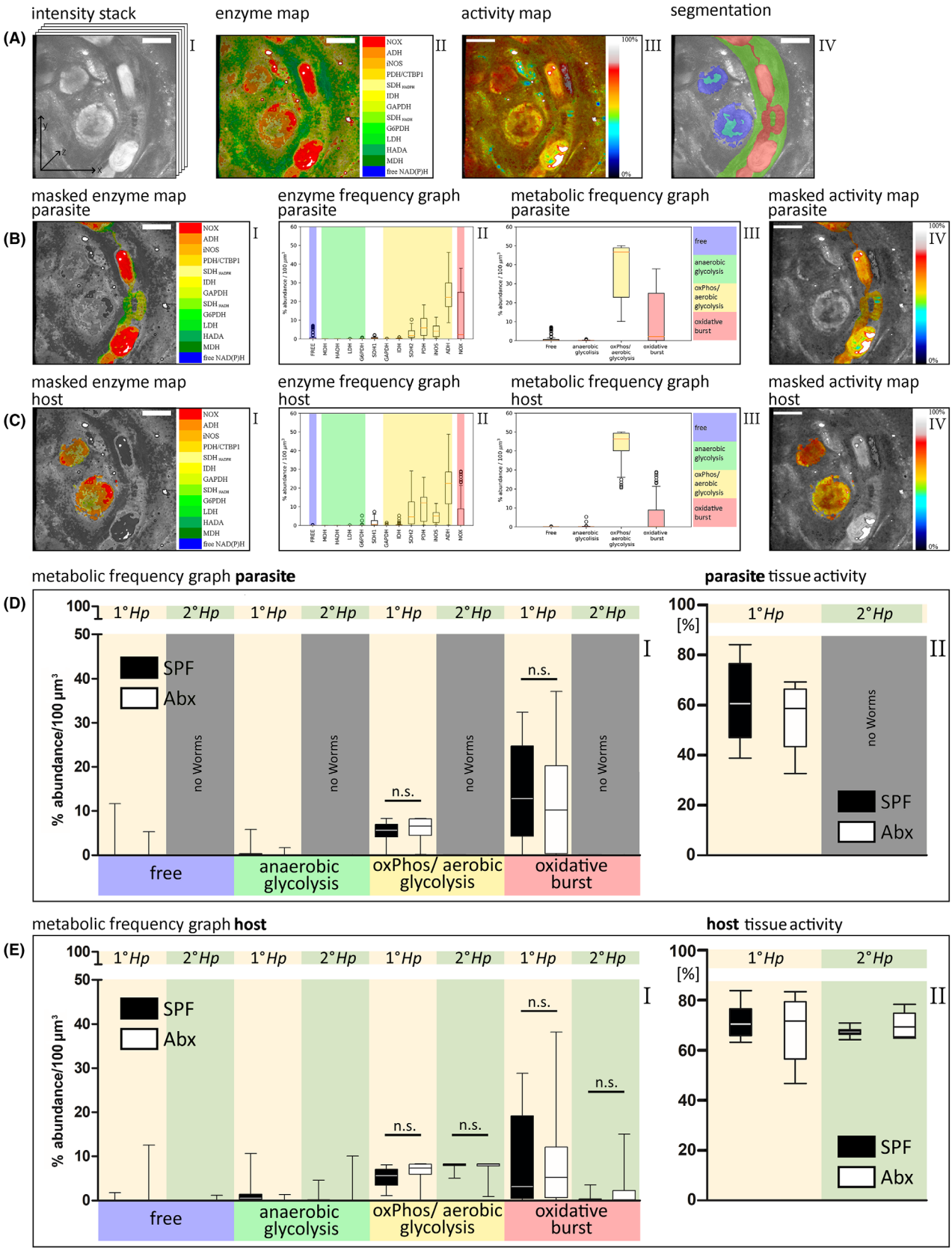

FIGURE 5 Legend on next page.

Using this analysis strategy, we found that in both nematodes and host tissue, the energy is mainly produced by aerobic glycolysis/oxPhos, independent of Abx treatment (Figure 5D,E, each I). Due to effective drug treatment, the number of nematodes after 2° Hp infection was very low and thus was insufficient for a reliable analysis. Furthermore, we did not find any change in NOX/DUOX-associated defence via oxidative burst, neither in host tissue nor in nematodes, with or without Abx (Figure 5D,E, each I). Only the NOX-associated defence appears to be lower in the gut tissue of the host after 2° Hp infection, as compared to 1° Hp infection. However, this finding needs to be confirmed and the underlying mechanisms need further investigation in future studies. The general metabolic activity in nematodes (Figure 5D, II) and host villi (Figure 5E, II) stays also unchanged, being slightly higher in host (≈70%) as compared to nematodes (≈60%) for all conditions.

4 | DISCUSSION

Placing the focus on the complex tripartite signalling, coordination and regulation between host, microbiota and parasite, numerous studies over the years have used germ-free mice as a platform to characterize the importance of gut commensals for effective immune responses against parasitic nematodes.[2,3,7,21–23] To expand on this, here we focused on applying a prolonged antibiotic treatment regimen over a total of 14 weeks in order to delineate what effects temporary abrogation of the host microbiota has on the development, maintenance and functionality of effector and memory Th2 responses following primary *H. polygyrus* infection, drug cure and challenge infection. In accordance with other studies,[2,24] we could confirm that prolonged administration of a cocktail of antibiotics in the drinking water is an effective strategy to temporarily remove the intestinal microbiota of mice, evidenced by the lack of detectable total Eubacteria DNA in faecal samples of Abx treated mice. Commensal bacteria have been shown to benefit the survival and persistence of several intestinal nematode species.[5,25–27] During *H. polygyrus* infection, experimental enrichment of rodent *Lactobacillaceae* and *Enterobacteriaceae* families coupled with the reduction of *Eubacterium/Clostridium* species through short Abx treatment, proved to increase adult worm load in a naturally *H. polygyrus*-resistant mouse strain.[27] Here, however, we demonstrate that complete removal of gut bacterial loads via prolonged Abx treatment has a slight positive effect on *H. polygyrus* colonization only during secondary infection. One potential explanation for this could be slower intestinal motion associated with reduced bacterial loads triggered by prolonged Abx treatment.[4]

Interestingly, in this study, and in contrast to previous studies,[2,3] we could not detect a difference in either worm count or egg numbers after 14 days of primary infection. Potentially, the more axenic model of *H. polygyrus* infection used by Rausch et al. (2018) and Russell et al. (2020) at 14 days via inoculation of germ-free mice limits the regulation of Th2 response in primary infected mice, leading to reduced egg numbers shed by female worms. In fact, both studies show increased Th2 immunity against *H. polygyrus* in germ-free mice, while here we detect no difference in Th2 immunity between SPF and Abx mice. Thus, this demonstrates that complete lack of microbiota potentiates Th2 response against parasitic helminths, while microbiota inherent

FIGURE 5 NAD(P)H fluorescence lifetime imaging in villi and nematodes during acute infection with *Heligmosomoides polygyrus*. (A, I) representative time-resolved NAD(P)H fluorescence intensity image of the duodenum and parasite in a C57/BL6 mouse acquired as a TCSPC-stack (time bin = 55 ps), 505 × 505 pixel ×227 time bins. The image shows a tissue layer in 58 μm depth within a 3D volume of 500 × 500 × 300 μm^3 (505 × 505 × 151 voxel). (A, II) Image generated from the processed NAD(P)H-FLIM data and the calculated fluorescent lifetimes using the phasor approach representing the predominant activity of NAD(P)H-dependent enzymes in each pixel. (A, III) Activity map representing the general metabolic activity, that is, the ratio of free to enzyme-bound NAD(P)H. (A, IV) Result of tissue segmentation in the NAD(P)H-fluorescence intensity image using a U-Net algorithm, used as masks for host (blue label), for entire nematode (green label) and high NAD(P)H-fluorescence signal in the parasite (red label). The segmentation is based on the intensity and spatial information (brightness, shapes and edges) criteria. Scale bar = 100 μm. (B, I) enzyme map in parasite tissue only, generated after masking the original enzyme map with the segmented regions of high NAD(P)H-signal in the parasite (red label in (A, V)). (B, II) Pixel frequencies of preferential enzyme activity, for each of the most abundantly expressed enzymes in parasites, normalized to 100 μm^3 tissue area. (B, III) Pixel frequencies for free NAD(P)H (no metabolic activity, blue) and the following metabolic pathways: anaerobic glycolysis-like (green), aerobic glycolysis/osPhos-like (yellow) as well as NOX/DUOX-dependent oxidative burst (red), as they result from clustering the enzyme activities in (B, II). (B, IV) Masked activity map in parasite tissue only describing the general metabolic activity in this. (C, I) Enzyme map in host villi only, generated after masking the original enzyme map with the segmented villi (blue label in (A, IV)), similar to (B). (C, II) Pixel frequencies of preferential enzyme activity, for each of the most abundantly expressed enzymes in villi, normalized to 100 μm^3 tissue area. (C, III) Pixel frequencies for free NAD(P)H (no metabolic activity, blue) and the following metabolic pathways: anaerobic glycolysis-like (green) and aerobic glycolysis/oxPhos-like (yellow) as well as NOX/DUOX-dependent oxidative burst (red), as they result from clustering the enzyme activities. (C, IV) Masked activity map in host tissue (villi) only describing the general metabolic activity. (D, I) Graph of metabolic frequency per dominant metabolic pathways (D, I) for nematode tissue, during 1st infection at day 14 (1° Hp), with (Abx, white) and without (SPF, black) antibiotic treatment. The number of nematodes analysed are for SPF 1°Hp $n = 6$ (6 mice) and for Abx 1°Hp $n = 14$ (5 mice). During 2° infection, we could not detect any worms in the intestinal tissue of the host and indicated this fact in the graph. (D, II) Metabolic activity for segmented parasite tissue under the analysed infection/treatment conditions. (E, I) Graph of metabolic frequency per dominant metabolic pathways for host tissue. Number of analysed duodenum regions are SPF 1°Hp $n = 10$ (6 mice), SPF 2°Hp $n = 6$ (1 mouse), Abx 1°Hp $n = 11$ (5 mice), Abx 2°Hp $n = 5$ (2 mice). Two independent experiments for 1st infection, with/without Abx treatment and an experiment for 2nd infection, with/without Abx treatment. (E, II) Metabolic activity for segmented host tissue under the analysed infection/treatment conditions. Statistical analysis was performed using two-way ANOVA test. $^*p \le .05$, $^{**}p \le .01$, $^{***}p \le .001$

from helminth larvae could still provide a modulatory environment for Th2 immune responses during primary infection in Abx treated mice.

Indeed, similar to the results presented here, Moyat et al. recently demonstrated that during primary *H. polygyrus* infection, Abx-treated mice harboured similar number of worms and eggs as SPF mice and only increased levels of IL-13 and total IgE and IgG1 were found in serum. Other immunological parameters, such as frequencies of IL-4 and IL-13 producing $CD4^+$ T cells in mLN as well as frequencies of tuft cells and mucus-producing goblet cells remained unaffected.[4] Similarly, in this study we did not detect significant differences in frequencies of circulating and tissue-resident effector and memory $Gata3^+$ Th2 cells on cured and challenged *H. polygyrus* mice, but we could notice a significant reduction of adult worm burden and female worm fecundity during secondary infection, compared with primary infection in either SPF or Abx mice. Previous studies performed in SPF mice have demonstrated similar protection against *H. polygyrus* challenge infection.[8,28] Thus, we were able to additionally show that prolonged antibiotic treatment and hence temporary removal of the host gut microbiome has no considerable effect neither on the formation, maintenance and functionality of memory Th2 cell responses following drug-cure of primary *H. polygyrus* infection, nor on host recall Th2 responses following secondary nematode infection. This therefore highlights the significant robustness of host Th2 responses against parasitic nematodes in relation to gut microbiota composition. However, whether the results presented here might differ, in terms of induction of stronger memory Th2 immune response during challenge infection when using germ-free larvae or reduced housing density of mice in cages, remains to be elucidated.[29,30]

On the other hand, to explain the significantly elevated HES-specific IgE titres in Abx mice compared to SPF mice during memory phase, we refer to a previous report showing spontaneous production of natural IgE in germ-free mice during steady state.[31] We believe that microbiota abrogation potentially can lead to overt sensitization of Abx mice to nematode-induced allergens and thus to the increase in IgE levels during the memory phase, thus in accordance with other studies that show that systemic allergic sensitization and oral challenge with OVA led to the serum induction of OVA-specific IgE, IgG1, IgG2a and IgA in germ-free mice compared to conventional mice.[32,33]

Beyond immune cell signalling and modulation, the complex relationship between host, microbiota and worm involves interspecies metabolic interactions, including compositional shifts in enzymes, metabolites and other nutrients.[34–37] Along this line, we therefore investigated whether prolonged antibiotic treatment affects general NAD(P)H-dependent metabolic activity and enzyme activity associated with specific metabolic pathways, both in the mouse intestine and in *H. polygyrus*. Using NAD(P)H fluorescence lifetime imaging (FLIM) in freshly explanted duodenum of infected mice, with and without antibiotic treatment, we confirmed a slightly higher general metabolic activity in host villi as compared to the parasites.[12] The energy production both in host and nematodes mainly follows metabolic pathways resembling aerobic glycolysis, rather than anaerobic glycolysis or β-oxidation of fatty acids (preferential activity of hydroxyacyl-coenzyme-A dehydrogenase—HADH), independent of antibiotic treatment. In line with the regulatory effect of nematode infection on the host immune system, we found the NOX/DUOX-related defence (oxidative burst capacity) to be lower after the 2° Hp infection as compared to the 1° Hp infection in intestinal tissue, independent of antibiotic treatment. Additionally, the NOX/DUOX-related defence (oxidative burst capacity) is independent of antibiotic treatment both in 1° and 2° Hp infection in the intestinal tissue. This parameter appears to be lower after the 2° Hp infection as compared to the 1° Hp infection, possibly resembling the regulatory effect of nematodes on the host immune system. However, this assumption needs to be confirmed in future studies.

In conclusion, both the metabolic pathways used for energy production and those used for defence relying on oxidative stress did not appear affected during prolonged antibiotic treatment, in host villi and in nematodes, in agreement with the lack of Abx treatment effects on host control of primary and secondary infection, as well as on the formation, maintenance or functionality of effector and memory Th2 cells. Our study therefore demonstrates that host Th2 immune responses and metabolic pathways are robust and remain independent of temporary experimental removal of the host gut microbiota following prolonged antibiotic treatment. However, whether, the host immune response-parasite interplay shown here after removal of intestinal microbiota behaves similar when using the same mouse strain but opposite sex,[38] warrants further investigation.

AUTHOR CONTRIBUTIONS

Ivet A. Yordanova, Raluca Niesner and Susanne Hartmann planned and designed the study. Luis E. Elizalde-Velázquez, Ivet A. Yordanova, Wjatscheslaw Liublin, Joshua Adjah, Ruth Leben and Sebastian Rausch performed the experiments, data analysis and interpretation. Luis E. Elizalde-Velázquez, Ivet A. Yordanova, Wjatscheslaw Liublin, Joshua Adjah, Ruth Leben, Raluca Niesner and Susanne Hartmann wrote the manuscript. Sebastian Rausch, Raluca Niesner and Susanne Hartmann supervised the study. All authors contributed to the article and approved the submitted version.

ACKNOWLEDGEMENTS

The authors would like to thank Yvonne Weber, Marion Müller, Bettina Sonnenburg, Christiane Palissa, Beate Anders and Robert Günther for providing excellent technical support. Open Access funding enabled and organized by Projekt DEAL.

FUNDING INFORMATION

This study was supported by a German Research Foundation (DFG) grant HA 2542/8-1 and HA 2542/12-1 awarded to SH, grant NI 1167/7-1 to RN, and GRK 2046 project B4 to SH and B5 to SR.

CONFLICT OF INTEREST

The authors declare that the research was conducted in the absence of any commercial or financial relationships that could be construed as a potential conflict of interest.

PEER REVIEW

The peer review history for this article is available at https://publons.com/publon/10.1111/pim.12957.

DATA AVAILABILITY STATEMENT

The data that support the findings of this study are available from the corresponding author upon reasonable request.

REFERENCES

1. Oh JZ, Ravindran R, Chassaing B, Carvalho FA, Maddur MS, et al. TLR5-mediated sensing of gut microbiota is necessary for antibody responses to seasonal influenza vaccination. *Immunity*. 2014;41(3):478-492. doi:10.1016/j.immuni.2014.08.009
2. Rausch S, Midha A, Kuhring M, et al. Parasitic nematodes exert antimicrobial activity and benefit from microbiota-driven support for host immune regulation. *Front Immunol*. 2018;9:2282. doi:10.3389/fimmu.2018.02282
3. Russell GA, Faubert C, Verdu EF, King IL. The gut microbiota limits Th2 immunity to *Heligmosomoides polygyrus* bakeri infection. *bioRxiv*. 2020. doi:10.1101/2020.01.30.927111
4. Moyat M, Lebon L, Perdijk O, et al. Microbial regulation of intestinal motility provides resistance against helminth infection. *Mucosal Immunol*. 2022:1-13. doi:10.1038/s41385-022-00498-8
5. Holzscheiter M, Layland LE, Loffredo-Verde E, Mair K, Vogelmann R, et al. Lack of host gut microbiota alters immune responses and intestinal granuloma formation during schistosomiasis. *Clin Exp Immunol*. 2014;175(2):246-257. doi:10.1111/cei.12230
6. Reynolds LA, Harcus Y, Smith KA, et al. MyD88 signaling inhibits protective immunity to the gastrointestinal parasite *Heligmosomoides polygyrus*. *J Immunol*. 2014;193(6):2984-2993. doi:10.4049/jimmunol.1401056
7. Ohnmacht C, Park JH, Cording S, et al. The microbiota regulates type 2 immunity throught ROR©t+ T cells. *Science*. 2015;349(6251):989-993. doi:10.1126/science.aac4263
8. Steinfelder S, Rausch S, Michael D, Kühl AA, Hartmann S. Intestinal helminth infection induces highly functional resident memory $CD4^+$ T cells in mice. *Eur J Immunol*. 2017;47(2):353-363. doi:10.1002/eji.201646575
9. Yordanova IA, Jürchott K, Steinfelder S, et al. The host peritoneal cavity harbors prominent memory Th2 and early recall responses to an intestinal nematode. *Front Immunol*. 2022;13:842870. doi:10.3389/fimmu.2022.842870
10. Harvie M, Camberis M, Tang SC, Delahunt B, Paul W, le Gros G. The lung is an important site for priming CD4 T-cell-mediated protective immunity against gastrointestinal helminth parasites. *Infect Immun*. 2010;78(9):3753-3762. doi:10.1128/IAI.00502-09
11. Obata-Ninomiya K, Ishiwata K, Nakano H, et al. $CXCR6^+ST2^+$ memory T helper 2 cells induced the expression of major basic protein in eosinophils to reduce the fecundity of helminth. *Proc Natl Acad Sci U S A*. 2018;115(42):E9849-E9858. doi:10.1073/pnas.1714731115
12. Liublin W, Rausch S, Leben R, et al. NAD(P)H fluorescence lifetime imaging of live intestinal nematodes reveals metabolic crosstalk between parasite and host. *Sci Rep*. 2022;12(1):7264. doi:10.1038/s41598-022-10705-y
13. Barman M, Unold D, Shifley K, et al. Enteric salmonellosis disrupts the microbial ecology of the murine gastrointestinal tract. *Infect Immunol*. 2008;76(3):907-915. doi:10.1128/IAI.01432-07
14. Leben R, Köhler M, Radbruch H, Hause AE, Niesner RA. Systematic enzyme mapping of cellular metabolism by phasor-analyzed label-free NAD(P)H fluorescence lifetime imaging. *Int J Mol Sci*. 2019;20(22):5565. doi:10.3390/ijms20225565
15. Madhukar NS, Warmoes MO, Locasale JW. Organization of enzyme concentration across the metabolic network in cancer cells. *PLoS One*. 2015;10(1):e0117131. doi:10.1371/journal.pone.0117131
16. Hewitson JP, Harcus Y, Murray J, et al. Proteomic analysis of secretory products from the model gastrointestinal nematode *Heligmosomoides polygyrus* reveals dominance of venom allergen-like (VAL) proteins. *J Proteomics*. 2011;74(9):1573-1594. doi:10.1016/j.jprot.2011.06.002
17. Chapman TJ, Pham M, Bajorski P, Pichichero ME. Antibiotic use and vaccine antibody levels. *Pediatrics*. 2022;149(5):e2021052061. doi:10.1542/peds.2021-052061
18. Haile AF, Woodfint RM, Kim E, et al. Broad-spectrum and gram-negative-targeting antibiotics differentially regulate antibody isotype responses to injected vaccines. *Vaccine*. 2021;9(11):1240. doi:10.3390/vaccines9111240
19. Uchiyama R, Chassaing B, Zhang B, Gewirtz AT. Antibiotic treatment suppresses rotavirus infection and enhances specific humoral immunity. *J Infect Dis*. 2014;210(2):171-182. doi:10.1093/infdis/jiu037
20. Murai A, Kitahara K, Okumura S, Kobayashi M, Horio F. Oral antibiotics enhance antibody responses to keyhole limpet hemocyanin in orally but not muscularly immunized chickens. *Anim Sci J*. 2016;87(2):257-265. doi:10.1111/asj.12424
21. Przyjalkowski Z, Krzysztyniak K, Golinska Z, Cabaj W, Konty E. Reactivity of lymphocytes in germfree and conventional mice infected with *Trichinella spiralis*. *Bull Acad Pol Sci Biol*. 1980;28(1–2):111-116.
22. Martins WA, Melo AL, Nicoli JR, Cara DC, Carvalho MAR, et al. A method of decontaminating *Strongyloides venezuelensis* larvae for the study of strongyloidiasis in germ-free and conventional mice. *J Med Microbiol*. 2000;49(4):387-390. doi:10.1099/0022-1317-49-4-387
23. White EC, Houlden A, Bancroft AJ, et al. Manipulation of host and parasite microbiotas: survival strategies during chronic nematode infection. *Sci Adv*. 2018;4(3):eaap7399. doi:10.1126/sciadv.aap7399
24. Kennedy MHE, Brosschot TP, Lawrence KM, FitzPatrick R, Lane JM, et al. Small intestinal levels of the branched short-chain fatty acid isovalerate are elevated during infection with *Heligmosomoides polygyrus* and can promote helminth fecundity. *Infect Immun*. 2021;89(12):e0022521. doi:10.1128/IAI.00225-21
25. Dea-Ayuela MA, Rama-Iniguez S, Bolas-Fernandez F. Enhanced susceptibility to *Trichuris muris* infection of B10Br mice treated with the probiotic *lactobacillus casei*. *Int Immunopharmacol*. 2008;8(1):28-35. doi:10.1016/j.intimp.2007.10.003
26. Hayes KS, Bancroft AJ, Goldrick M, Portsmouth C, Roberts IS, Grencis RK. Exploitation of the intestinal microflora by the parasitic nematode *Trichuris muris*. *Science*. 2010;328(5984):1391-1394. doi:10.1126/science.1187703
27. Reynolds LA, Smith KA, Filbey KJ, et al. Commensal-pathogen interactions in the intestinal tract: lactobacilli promote infection with, and are promoted by, helminth parasites. *Gut Microbes*. 2014;5(4):522-532. doi:10.4161/gmic.32155
28. Ekkens MJ, Liu Z, Liu Q, et al. Memory Th2 effector cells can develop in the absence of B7-1/B7-2, CD28 interactions, and effector Th cells after priming with an intestinal nematode parasite. *J Immunol*. 2002;168(12):6344-6351. doi:10.4049/jimmunol.168.12.6344
29. Russell GA, Peng G, Faubert C, Verdu EF, Hapfelmeier S, King IL. A protocol for generating germ-free *Heligmosomoides polygyrus* bakeri larvae for gnotobiotic helminth infection studies. *STAR Protoc*. 2021;2(4):100946. doi:10.1016/j.xpro.2021.100946
30. Russell A, Copio JN, Shi Y, Kang S, Franklin CL, Ericsson AC. Reduced housing density improves statistical power of murine gut microbiota studies. *Cell Rep*. 2022;39(6):110783. doi:10.1016/j.celrep.2022.110783
31. McCoy KD, Harris NL, Diener P, Hatak S, Odermatt B, et al. Natural IgE production in the absence of MHC class II cognate help. *Immunity*. 2006;24(3):329-339. doi:10.1016/j.immuni.2006.01.013
32. Schwarzer M, Srutkova D, Hermanova P, Leulier F, Kozakova H, Schabussova I. Diet matters: endotoxin in the diet impacts the level of allergic sensitization in germ-free mice. *PLoS One*. 2017;12(1):e0167786. doi:10.1371/journal.pone.0167786
33. Schwarzer M, Hermanova P, Srutkova D, et al. Germ-free mice exhibit mast cells with impaired functionality and gut homing and do not develop food allergy. *Front Immunol*. 2019;10:205. doi:10.3389/fimmu.2019.00205
34. Cortes-Selva D, Fairfax K. Schistosome and intestinal helminth modulation of macrophage immunometabolism. *Immunology*. 2021;162(2):123-134. doi:10.1111/imm.13231

35. Reynolds LA, Redpath SA, Yurist-Doutsch S, et al. Enteric helminths promote *Salmonella* coinfection by altering the intestinal metabolome. *J Infect Dis*. 2017;215(8):1245-1254. doi:10.1093/infdis/jix141
36. Hu Y, Chen J, Xu Y, et al. Alterations of gut microbiome and metabolite profiling in mice infected by *Schistosoma japonicum*. *Front Immunol*. 2020;11:569727. doi:10.3389/fimmu.2020.569727
37. Cattadori IM, Sebastian A, Hao H, et al. Impact of helminth infections and nutritional constraints on the small intestinal microbiota. *PLoS One*. 2016;11(7):e0159770. doi:10.1371/journal.pone.0159770
38. Elderman M, de Vos P, Faas M. Role of microbiota in sexually dimorphic immunity. *Front Immunol*. 2018;9:1018. doi:10.3389/fimmu.2018.01018

SUPPORTING INFORMATION

Additional supporting information can be found online in the Supporting Information section at the end of this article.

How to cite this article: Elizalde-Velázquez LE, Yordanova IA, Liublin W, et al. Th2 and metabolic responses to nematodes are independent of prolonged host microbiota abrogation. *Parasite Immunol*. 2023;45(4):e12957. doi:10.1111/pim.12957